Ultimate limit state of spread foundation on sand during earthquake

Hideyuki Mano[1]

[1] Construction Technology Dept., Shimizu Corporation, 2-16-1, Kyobashi, Chuo-ku, Tokyo, 104-8370, Japan

ABSTRACT

To investigate the ultimate limit states of a spread foundation on sand during earthquake, model experiments were performed in which loading was applied in the order: vertical force, horizontal force, and vertical force. The ultimate limit states of the spread foundation under horizontal loading are sliding or overturning, revealing that failure by load inclination did not occur. The ultimate vertical bearing capacity of the spread foundation, in which it does not cause sliding or overturning, is approximately the same as that under the pure vertical loading.

Keywords: bearing capacity, horizontal load, overturning, sliding, shallow foundation

1 INTRODUCTION

In addition to vertical loads, horizontal loads and overturning moments act on spread foundations during an earthquake. To analyze the vertical bearing capacity of spread foundations subjected to combined loads, evaluation methods that employ an eccentric and inclined load have been proposed (Meyerhof, 1953). According to this proposal, if the seismic force is large, the ultimate vertical bearing capacity may be smaller than the self-weight of the structure.

In the 1995 Southern Hyogo Prefecture Earthquake, ground surface acceleration of more than 800 cm/s^2 was observed. However, on flat ground that did not liquefy, there was no reported damage to spread foundations in the damage survey (Maruoka et al. 1997). Shaking table tests of structures with spread foundations on sand, receiving strong earthquakes have been performed, and it was reported that both the residual inclination and settlement of the foundation were small (Shirato et al. 2008).

Meyerhof's proposed formula is in good agreement with the analysis and experimental results for spread foundations, in which eccentric inclined loads have been applied. However, as mentioned above, it is in poor agreement with the observed earthquake damages and model vibration experiment results. This disagreement is thought to be caused by the replacement of the combined loads with an eccentric inclined load. In this study, static loading model experiments simulating the load condition at the time of earthquake of a structure on sand were performed. Based on the experimental results, the ultimate limit state of the spread foundations receiving combined loads was discussed.

2 ULTIMATE LIMIT STATE OF A SPREAD FOUNDATION

Fig. 1 shows the method of replacing the combined loads with an eccentrically inclined load, while Fig. 2 shows the failure surface of overturning and sliding. If the inclination angle of the load, θ is not zero, the failure surface extends toward the loading direction from the rear end of the effective foundation width which is reduced by the overturning moment, regardless of the eccentric distance of the load, e. Therefore, overturning and sliding, shown in Fig. 2, cannot be explained by Meyerhof's proposal.

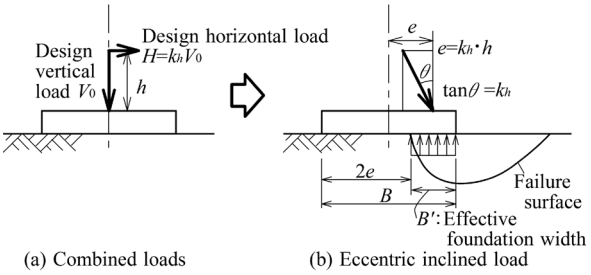

Fig. 1. Combined loads and eccentric inclined load.

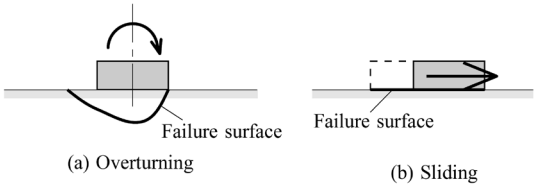

Fig. 2. Failure surface of overuturning and sliding.

3 EXPERIMENTAL OUTLINE

Model experiments were carried out by the sequential loading of vertical and horizontal forces to investigate the ultimate limit states of an actual building

during an earthquake. The experimental models comprised of spread foundations on sand, without embedment. The loading was performed in three steps, as shown in Fig. 3:

STEP 1: Apply the initial vertical load V_0 (= αV_u, V_u: ultimate vertical bearing capacity under pure vertical loading, α: vertical loading ratio $0 < \alpha \leqq 1$).

STEP 2: Apply the horizontal load H (= $k_h \cdot V_0$, k_h: planned horizontal seismic intensity) to height h. Horizontal load H and overturning moment M (= $k_h \cdot V_0 \cdot h$) act on the foundation.

STEP 3: If the ultimate state is not reached in STEP 2, apply the vertical load ΔV while maintaining the horizontal load H to achieve the ultimate state. The vertical bearing capacity is V_{max} (= $V_0 + \Delta V$).

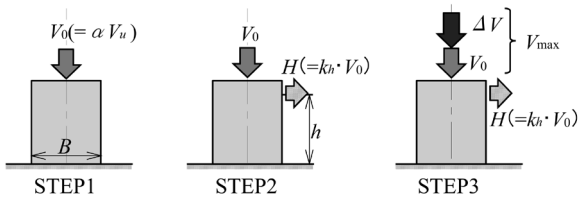

Fig. 3. Loading order.

The experimental model is shown in Fig. 4. The ground of the model was made of air-dried Toyoura sand with a target relative density Dr = 90% (ϕ = 45°). The model structure had a width of 100 mm (B) and a length of 100 mm (L). The height h at which the horizontal load was applied varied between the models; 20 mm (L series), 100 mm (M series), and 200 mm (H series). Toyoura sand was glued to the base of each model to simulate a rough footing base condition. A load cell, a spherical support, and a slider were employed in each structural model.

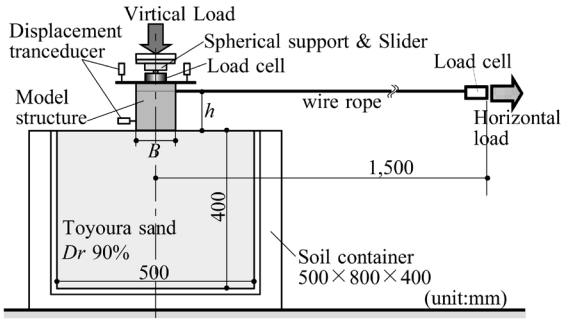

Fig. 4. Test apparatus.

The experimental cases are shown in Table 1. The experimental parameters were: height of applied horizontal force h, initial vertical load V_0, and planned horizontal seismic intensity k_h. Case L-0 was used to determine V_u. The rightmost column of the table shows the ultimate limit state in each experiment. In the case of M400-0.8, both sliding and overturning were considered to be the ultimate states.

Table 1. Experimental cases examined in this study.

Case	h/B	V_0 (N)	k_h	Ultimate limit state
L-0	-	2,952	0	V
L200-0.5		200	0.5	V
L200-0.8		200	0.8	S
L400-0.4		400	0.4	V
L400-0.8		400	0.8	S
L800-0.2	0.2	800	0.2	V
L800-0.4		800	0.4	S
L1600-0.1		1,600	0.1	V
L1600-0.2		1,600	0.2	V
L1600-0.3		1,600	0.3	S
M400-0.4		400	0.4	V
M400-0.8		400	0.8	O&S
M800-0.2		800	0.2	V
M800-0.3	1.0	800	0.3	V
M800-0.4		800	0.4	S
M1600-0.2		1,600	0.2	V
M1600-0.3		1,600	0.3	S
H200-0.5		200	0.5	O
H400-0.8		400	0.8	O
H800-0.15	2.0	800	0.15	V
H1000-0.5		1,000	0.5	O
H1600-0.1		1,600	0.1	V

V: Vertical bearing capacity, S: Sliding, O: Overturning

4 RESULTS AND DISCUSSIONS

The ultimate vertical bearing capacity V_u under pure vertical loading was 2,952 N. In the experiments, there were no cases in which a failure surface was formed in front of the foundation (as shown in Fig. 1 (b)). The following three ultimate states were observed:

(I) The foundation slid during horizontal force loading in STEP 2.

(II) The rotation of the foundation continued to increase without increasing the horizontal load in STEP 2. (overturning)

(III) In STEP 3, the vertical bearing capacity reached its limit.

4.1 Sliding in STEP 2

For the L and M series, all the cases that reached the ultimate state in STEP 2 ended with sliding. Fig. 5 shows the relationship between the horizontal load and the horizontal displacement, and rotation angle of the foundation for case M800-0.4. In the case of M800-0.4, only the horizontal displacement increased while the horizontal load was constant, so the ultimate limit state was sliding.

Fig. 6 shows the relationship between the horizontal seismic intensity k_h and the vertical load ratio V_0/V_u. The k_h at the commencement of sliding is hereinafter referred to as $k_{h\text{-}s}$. The horizontal seismic intensity at the commencement of sliding ($k_{h\text{-}s}$) corresponds to the friction coefficient μ. In previous studies that focused on the friction between the sand and construction materials in laboratory tests using simple shear type apparatus, it was found that the friction coefficient μ depended on the surface roughness of the bottom of the foundation and the shear resistance angle ϕ of the sand (Uesugi et al., 1986). However, in these experiments, $k_{h\text{-}s}$ (=μ) varied depending on the magnitude of V_0/V_u; the friction coefficient μ decreased as V_0/V_u increased. From Fig. 6, it can be seen that the relationship between V_0/V_u and $k_{h\text{-}s}$ (= μ) was in

good agreement with the inclination factor i_γ (Meyerhof 1953) for the vertical component of the bearing capacity under a load inclined at an angle of θ from the vertical. Since θ is equivalent to $\tan^{-1}k_{h\text{-}s}$ (= $\tan^{-1}\mu$), i_γ is expressed by Equation (1):

$$\frac{V_0}{V_u} = i_\gamma = \left(1-\frac{\theta}{\phi}\right)^2 = \left(1-\frac{\tan^{-1}k_{h-s}}{\phi}\right)^2 \qquad (1)$$

The results of the cases that overturned in STEP 2 or did not reach the ultimate state in STEP 2 are also shown in Fig. 6. All these points are located on the left side of the line of Equation (1).

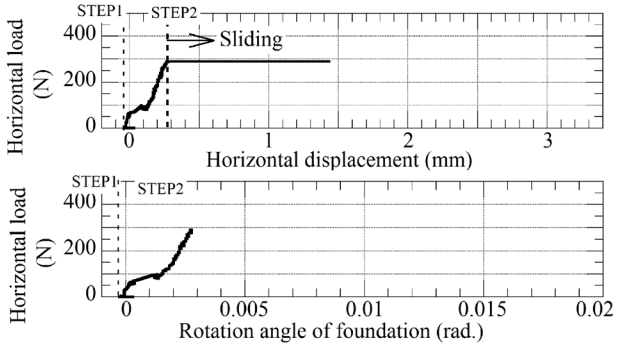

Fig. 5. The relationship between the horizontal load and horizontal displacement, rotation angle (M800-0.4).

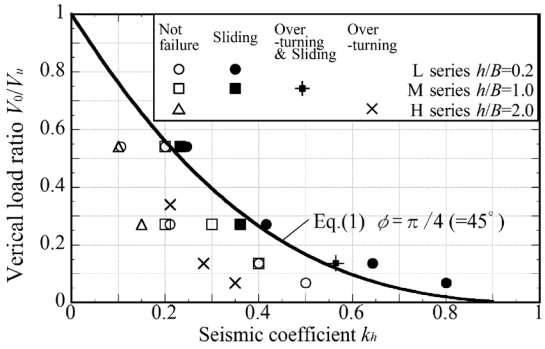

Fig. 6. The relationship between k_h and V_0/V_u.

4.2 Overturning in STEP 2

For case H400-0.8, Fig 7 shows the relationship between the horizontal load and horizontal displacement of the foundation, and the rotation angle of the foundation. After generating a small peak, the rotation angle continued to increase with an almost constant horizontal load. The increase in the horizontal displacement during this period was slight, thus the ultimate limit was considered to have been reached by overturning.

The ultimate resistance moment against overturning can be calculated using the concept of an effective width B' of a foundation, subject to an eccentric load (Meyerhof 1953). Fig. 8 shows the relationship between the eccentricity (e/B) of the resultant force of the contact pressure and V_0/V_u, obtained from Equations (2) - (4).

$$\frac{V_0}{V_u} = \frac{\beta'\gamma B' N_\gamma B' L}{\beta\gamma B N_\gamma B L}$$

$$= \left(1+\frac{0.8}{\frac{L}{B}-0.4}\cdot\frac{e}{B}\right)\left(1-2\frac{e}{B}\right)^2 \qquad (2)$$

$$B' = B - 2e \qquad (3)$$

$$\beta = 0.5 - 0.2\frac{B}{L} \qquad \beta' = 0.5 - 0.2\frac{B'}{L} \qquad (4)$$

γ: effective unit weight of soil
N_γ: bearing capacity factor

Fig. 8 also shows the results of the experiments performed by Fukui et al. (2007), where (B = L = 50 cm). Fukui's results agreed with the case shown by the solid line. Of the experiments carried out in the present study, the e/B values of the cases that overturned were greater than those represented by the solid line. They agreed well with the line obtained by multiplying e/B by 1.6 (dashed line). In the experiments performed by Fukui et al., the vertical load was given by the structural weight. On the other hand, in our experiments, the vertical load was applied by an electric jack to produce a larger load. In our experiments, jack operation was performed so that the vertical load was constant; however, it was impossible to completely eliminate the influence of the vertical displacement constraint by the jack. All cases that slid or did not reach the ultimate limit state in STEP 2 are on the left side of the dashed line.

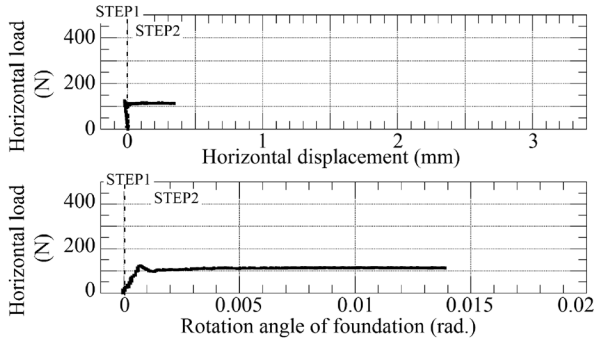

Fig. 7. The relationship between the horizontal load and horizontal displacement, rotation angle (H400-0.8).

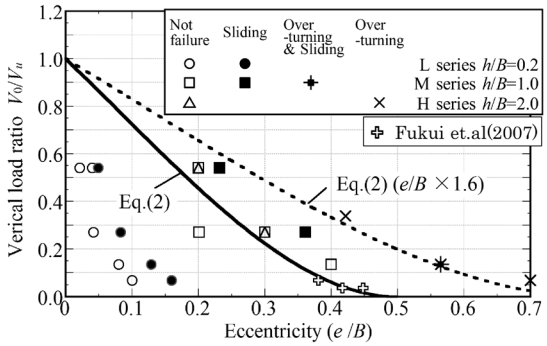

Fig. 8. The relationship between e/B and V_0/V_u.

4.3 Cases in which the vertical bearing capacity reached its ultimate limit in STEP 3

For cases in which the ultimate limit state was not reached in STEP 2, only the vertical loads were increased to reach the ultimate limit state, while the horizontal forces were maintained in STEP 3.

Fig. 9 shows a comparison of the vertical load - settlement relationship for cases L-0, L1600-0.2, M1600-0.2, and H1600-0.1. The settlements increased slightly during the horizontal forces were applied. In cases where the vertical load increased while maintaining the horizontal force, the load-settlement curve quickly returns to pure vertical loading. No significant differences were observed in the shapes of the load-settlement curves, and the ultimate vertical bearing capacities did not depend on the magnitude of the horizontal force and the overturning moment.

Fig 10 shows the relationship between the vertical loading ratio (V_0/V_u in STEP 2, V_{max}/V_u in STEP 3) and the horizontal seismic intensity k_h (H/V_0 in STEP 2, H/V_{max} in STEP 3). When only the vertical load increased in STEP 3, the vertical bearing capacity was not reduced and sliding did not occur, even when $(V_0+\Delta V)/V_u$ exceeded the curve of Equation (1). In all cases of STEP 3, the ultimate vertical bearing capacities were almost equal to V_u.

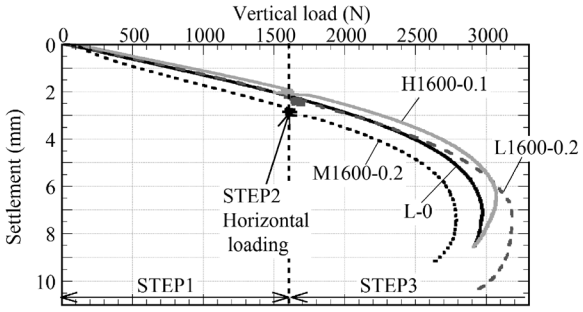

Fig. 9. The vertical load - settlement curves.

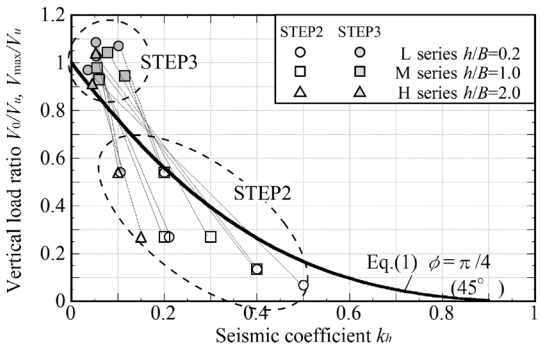

Fig. 10. The relationship between k_h and V_0/V_u, V_{max}/V_u.

5 DISCRIMINATION BETWEEN SLIDING AND OVERTURNING

Whether the ultimate limit state of a spread foundation, when a horizontal force and overturning moment are acting upon it, is overturning or sliding, is determined by which one requires a smaller horizontal force. Fig. 11 shows the relationship between h/B and V_0/V_u for the experiments in which sliding or overturning occurred in STEP 2. The boundary line between sliding and overturning was obtained by multiplying e/B by 1.6, according to the experimental results. The boundary line, shown in Fig. 11, was in good agreement with the experimental results, in which the ultimate limit states were changed not only by h/B, but also by V_0/V_u.

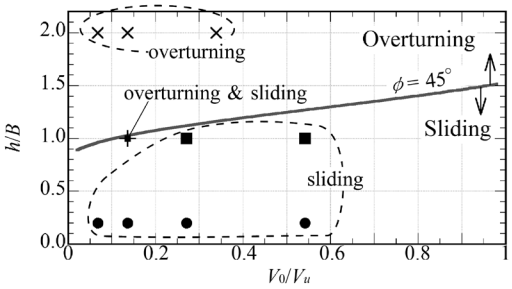

Fig. 11. Change in the ultimate limit state by in relation to h/B and V_0/V_u (comparison with experimental results).

6 CONCLUSIONS

The following conclusions were obtained with respect to the ultimate limit states of a spread foundation on sand, by the model experiments, in which the load conditions were divided into three steps simulating the actual load state of the building.

1) The ultimate limit states of a spread foundation subjected to horizontal loading are sliding or overturning. Failure due to load inclination does not occur.
2) The horizontal seismic intensity $k_{h\text{-}s}$, causing sliding, can be expressed by the formula of the supporting force reduction rate i_γ due to the inclined load.
3) If the ultimate limit state is not reached by the horizontal force and overturning moment, and only the vertical load increases relative to this state sliding and overturning do not occur. Even if a horizontal force or overturning moment is applied, the ultimate vertical bearing capacity of the spread foundation is approximately the same as that under the pure vertical loading.
4) The ultimate limit states (sliding or overturning) of a spread foundation with horizontal loading is determined from the foundation width, the height of the applied horizontal load, the shear resistance angle of the ground, and the vertical loading ratio.

REFERENCES

Fukui, J., Nakatani, S., Shirato, M., Kouno, T., Nonomura, Y. and Asai, R., (2007). Experimental study on residual displacement of shallow foundations during large earthquake, Technical Memorandum of PWRI, (4027), Public Works Research Institute, Tsukuba, Japan (in Japanese)

Maruoka, M., Aoki, M., Sato, E., Hirai, Y., Miyagawa, H. and Watanabe, T. (1997). Damage to building foundation during the 1995 Hyogoken-nanbu earthquake, AIJ J. of Technology and Design 5, 85-90 (in Japanese)

Meyerhof, G. G. (1953). The bearing capacity of foundations under eccentric and inclined loads. Proc. 3rd Int. Conf. Soil Mech. and Foundation Engineering, 440-445

Shirato, M., Kohno, T., Asai, R., Nakatani, S., Fukui, J., Paolucci, R. (2008). Large-scale Experiments on Nonlinear Behavior of Shallow Foundations Subjected to Strong Earthquakes, Soils and Foundations 48(5), 673-692

Uesugi, M., Kishida, H. (1986). Frictional resistance at yield between dry sand and mild steel, Soils and Foundations 26(4), 139-148